‘Inductance’ definitions, modeling, and simulation

Yivgeni Semidotskih, Evgeny Rozanov, Hermann Haag, Florian Haemmerle
and Shmuel (Sam) Ben-Yaakov, *Life Fellow, IEEE*

***Abstract* - The nonlinear behavior of the B-H relationship of a ferromagnetic material gives rise to two different types of permeabilities: ‘total permeability’ and ‘derivative permeability’. These are used in this study to define three inductances of a current dependent inductor that is built around a ferromagnetic core: ‘total inductance’, ‘derivative inductance’ and ‘energy related inductance’. The latter is the correct parameter to be used when calculating the energy stored in a current dependent inductor. Based on these inductance definitions, state equations for the various ‘inductances’ were developed and used to implement SPICE compatible models by applying behavioral dependent sources. The theoretical derivations of this work were validated by simulation and experimentally.**

I. Introduction

Power inductors are widely used in power electronics systems. Many, if not most, of the inductors are built around a ferromagnetic core which exhibits a non-linear B-H characteristic. Consequently, the inductance of power inductors is generally a non-linear function of the current passing through them. Hence, when simulating a power electronics system, one has often to include models of current dependent inductors to closely emulate the behavior of the system. SPICE models of current dependent inductors are thus important for theoretical investigations as well as for the examination and tuning of engineering designs. SPICE based simulation tools are very popular among workers in the power electronics field due to them being readily available, user friendly and quick to setup and run. This paper is focused on SPICE modeling and does not intend to provide a general overview of variable inductors modeling tools. Furthermore, this paper concentrates on global behavioral models [1-4] as opposed to structural, reluctance type, models [5].

Despite the many previous publications that apply non-linear inductor models and demonstrate their applications in analysis and simulation, there seems to be a confusion as to the differences between the models and which model is appropriate for any given case. For example, in [6], page 302, equation10.2 and in [7] the authors state that the proper model for a current dependent inductor is:

$$v = L(i)\frac{di}{dt} + i\frac{d(L(i))}{dt} \qquad (1)$$

where i is the inductor’s current, $L(i)$ is the inductance as a function of current, and v is the voltage across the inductor. Judging from the discussion that follows (e.g. Fig. 10.2, Fig. 10.4, Fig. 10.5, in [6]) it is understood that what is meant by $L(i)$ is the *incremental inductance* (defined in this paper as $L_d(i)$). That is, the inductance per the incremental permeability at a given current. However, as will be discussed in the following, equation (1) is relevant to the *total inductance* (defined in this paper as $L_t(i)$), and not the incremental or derivative inductance as wrongly done in [6, 7].

Previous publications have demonstrated that once a SPICE model of a variable inductor is calibrated against experimental data, it yields accurate results in mimicking the inductor’s behavior under static and dynamic conditions. However, the apparent lack of clarity as to the differences between the previously proposed models, calls for formal classification of the many SPICE modeling alternatives.

The objective of this paper is to delineate the meaning of ‘inductance’, to define the various ‘inductances’ and their corresponding state equations, and to present the fundamentals of SPICE modeling of current dependent inductors. The work follows the concepts developed earlier in connection with voltage dependent capacitors [8]. This study concentrates on the average behavioral approach and does not include the modeling of the B-H hysteresis effect, nor does it address the issue of core losses or winding losses.

II. The definitions of 'inductance'

It would appear that some of the inconsistencies in the choice of current dependent inductors models stems from not properly defining the 'inductance' in use. The proper definition of inductance hinges on the proper definition of permeability μ since the inductance of a physical inductor is related to the permeability, μ, by a constant

$$L = K_l\mu \qquad (2)$$

As discussed below, μ can be defined in several ways which brings about different definitions to the inductance L. In the following, the notation ‘i’ (lower case) is used to designate a variable current while ‘I’ (upper case) is used for a specific, fixed, current.

Given a nonlinear ferromagnetic material, the relationship between the magnetic field (H) and the magnetic flux density (B) is, in general, non-linear, as illustrated in Fig. 1 for the first quadrant. It should be noted that the general representation of Fig. 1 is valid both for gapped and ungapped cores - the difference being the shape of the curves. Although μ is classically defined as B/H, there are, in fact, at least two particular forms that can be considered: total permeability and derivative permeability.

The formal, textbook, definition of inductance is based on total permeability μ_t (Fig. 1) defined as:

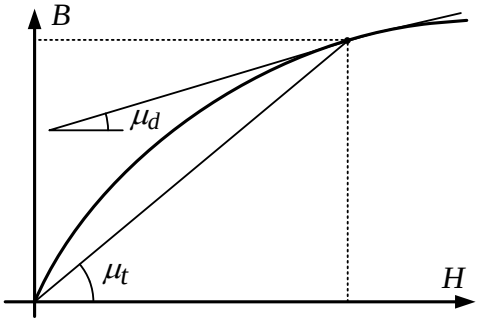

Fig. 1 Graphical illustration of "total permeability", μ_t, and "derivative permeability", μ_d.

$$\mu_t(H) = B/H \tag{3}$$

where H is the magnetic field and B is the magnetic flux density, which leads to the textbook definition of the inductance, in this case 'total inductance' L_t:

$$L_t(I) = n\Phi/I \tag{4}$$

where n is the number of turns and ϕ is the flux via the core, and I is the inductor's current.

Since

$$v = n\frac{\mathrm{d}\Phi}{\mathrm{dt}} \tag{5}$$

where v is the voltage across the inductor, this equation leads to:

$$v = \frac{d[i\,(L_t(i))]}{dt} \tag{6}$$

Hence, the state equation for total inductance L_t is:

$$v = L_t(i)\frac{di}{dt} + i\frac{d(L_t(i))}{dt} \tag{7}$$

However, the most popular definition of inductance, which is used widely in the industry and given in datasheets of commercial products, is the derivative, (or differential or incremental) inductance which is based on the derivative permeability (μ_d, Fig. 1). That is:

$$\mu_d = dB/dH \tag{8}$$

The state equation of the incremental inductance can be derived as follows. Starting from Faraday's Law

$$v = n\frac{d\Phi}{dt} \tag{9}$$

We find

$$v = nA\frac{\mathrm{dB}}{dt} \tag{10}$$

where A is the cross-section area of the core.

Equation (10) can be formulated as

$$v = nA\frac{\mathrm{dB}}{dH}\frac{\mathrm{dH}}{dt} \tag{11}$$

and hence:

$$v = \frac{n^2A\mu_d}{l}\,\frac{di}{dt} \tag{12}$$

where l is the magnetic path length.

This leads to the definition of the incremental inductance

$$L_d(I) = \frac{n^2A}{l}\mu_d(I) \tag{13}$$

And hence, from (12) the state equation of the incremental inductor is:

$$v = L_d(i)\,\frac{di}{dt} \tag{14}$$

The inductance $L_d(I)$ is very useful and is used, for example, when evaluating the ripple current in a PWM converter at a given inductor current.

Clearly, for a linear inductor, $L_t = L_d$ but for the general case of a nonlinear inductor, $L_t \neq L_d$. The relationship between the two can be found via the relevant permeabilities as follows:

$$\mu_d(H) = dB/dH \tag{15}$$

$$dB = \mu_d(H)dH \tag{16}$$

$$B = \int_0^H \mu_d(H)dH \tag{17}$$

$$\mu_t(H) = B/H \tag{18}$$

$$\mu_t(H) = \frac{\int_0^H \mu_d(H)dH}{H} \tag{19}$$

or:

$$\mu_t(I) = \frac{\int_0^I \mu_d(i)di}{I} \tag{20}$$

This translates into the relationship

$$L_t(I) = \frac{\int_0^I L_d(i)di}{I} \tag{21}$$

Another useful, and seemingly overlooked definition of inductance is 'energy related inductance' $L_e(i)$. That is, the 'inductance' value that need to be used when calculating the energy stored in a current dependent inductor at a given current. Clearly, the use of L_d and L_t for this purpose is incorrect. The expression for $L_e(I)$ can be derived by the formal definitions of electrical energy E and power P

$$\mathrm{P}=\frac{dE}{dt} = vi \tag{22}$$

From (14)

$$\frac{dE}{dt} = i\,L_d(i)\,\frac{di}{dt} \tag{23}$$

Hence

$$dE\ = i\,L_d(i)\,di \tag{24}$$

Defining $L_e(I)$ via

$$E(I) = \frac{I^2L_e(I)}{2} \tag{25}$$

we find

$$L_e(I) = \frac{2\int_0^I L_d(i)\,i\,di}{I^2} \tag{26}$$

For a linear inductor

$$L_e(I) = \frac{2L_d \int_0^I i\, di}{I^2} = L_d(I) = L_t(I) \qquad (27)$$

A typical behavior of the various "inductances" as obtained by the SPICE models detailed below for a demo inductor, is depicted in Fig. 2.

It is observed that the three inductances drop as a function of the bias current, as one would expect, but the values of the inductances are considerably different. The highest drop is observed for L_d because the derivative of the B/H curve is becoming very small as saturation is approached.

Another interesting observation that can be made by applying the analytical expressions derived above, is the error that will be encountered if the wrong inductance is used to calculate the energy stored in an inductor. Fig. 3 shows the values of the stored energy calculated by applying L_t, L_d or L_e. Clearly, the only correct curve is the one according to L_e. The error committed when applying the wrong inductance is very large, especially at a higher current when saturation is approached.

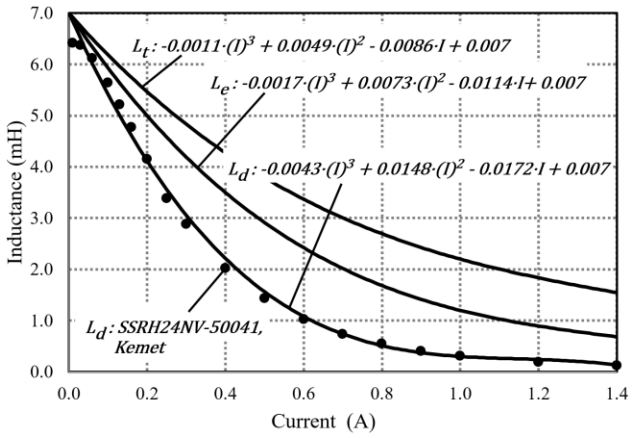

Fig. 2 Behavior of L_t, L_d and L_e of a demo inductor. Dots: measured, Lines: as obtained by the proposed SPICE models.

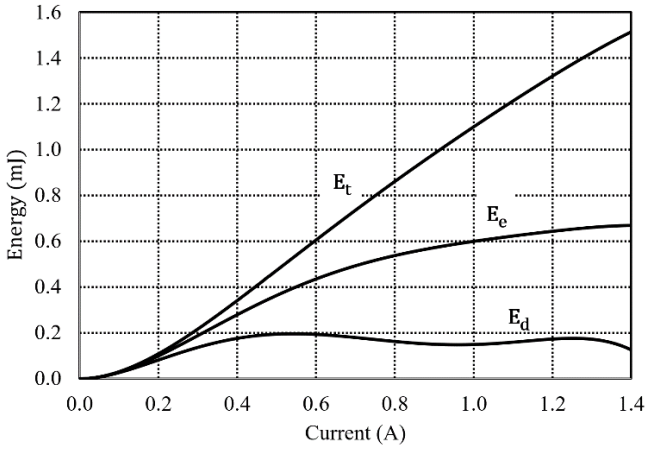

Fig. 3 Stored energy as calculated by using L_t (E_t), L_d (E_d) and L_e (E_e). Only the one calculated by Le is correct.

III. Possible SPICE models of current dependent inductors

Considering the above, there are a number of ways for devising a SPICE compatible model of a variable inductor. These can be divided into two groups: models that are based on L_t and those based on L_d. Some of the model implementations are discussed below.

A. Models based on L_t

A.1. Model A

The first SPICE compatible model of L_t to be considered (designated as Model A), follows the basic state equation that is based on L_t (7). This expression can be emulated by a voltage source equal to the sum of the two right terms. For that, there is a need to generate a SPICE compatible variable that mimics $L_t(i)$. This can be done by a behavioral model (such as EVALUE in PSPICE) in which the {expression} is an experimentally fitted equation of L_t as a function of *i*, and the numerical value of the output voltage is equal to the value of the $L_t(i)$. An example of a possible implementation of this model in PSPICE is given in Fig. 4.

The implementation shown in Fig. 4 applies a behavioral voltage sources (EVALUE, E1) and (EVALUE, E2) whose output signals are per the specified expression. The expression of E1 applies the derivative operator of PSPICE, DDT to implement (7). The output of E1 source, nodes L1, L2, are the terminals of the emulated inductor. The dependent voltage source E2, is used to generate the value of the inductance *Lt* as a function of the inductor current. That is, the value of the voltage at *Lt* is equal numerically to the value of the inductance. It is assumed, just for the sake of illustration, that $L_t(i)$ is given by an empirical equation that was found by fitting data points a polynomial equation.

$$L_t(i) = 0.007 - 0.0172 * |i| + 0.0148 * i^2 - 0.0043 * |i^3| \qquad (28)$$

The absolute operator (abs in Fig. 4) is required to handle both positive and negative voltages across the inductor. An alternative embodiment of the SPICE model according to Model A is to describe $L_t(i)$ as a Table [8] rather than as a fitted curve. The advantage of the table approach is that it includes the actual measured points. The downside is that it might cause errors and convergence problems due to the discrete nature of the data and the irregularity of the array, especially when derivate operators are used.

A.2. Model B

Following [8], another approach can be taken for implementing a SPICE $L_t(i)$ model. Based on the definition of $L_t(i)$, one can also get an integral form for the model as follows:

$$i(t) = \frac{\int_0^t v dt}{L_t(i)} \qquad (29)$$

That is, the implementation is by a current source rather than a voltage source (Fig.). This implementation makes use of the PSPICE integral operator SDT.

B. Models based on L_d

B.1. Model C

This model is a direct translation of the state equation (14) into a SPICE behavioral model (Fig. 6).

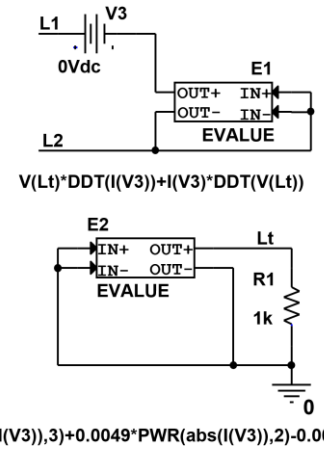

Fig. 4 Possible implementation of an $L_t(i)$ SPICE model according to (7) by a curve fitted equation.

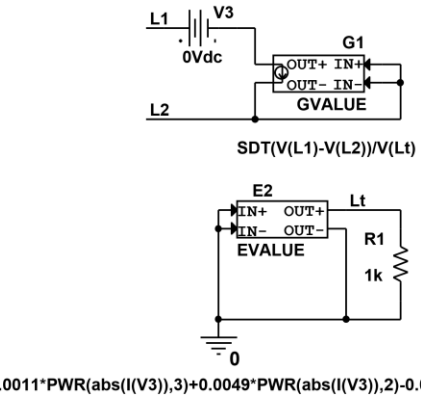

Fig. 5 PSPICE implementation of $L_t(i)$ by applying direct translation of (29) to a PSPICE expression using the integral (SDT) operator.

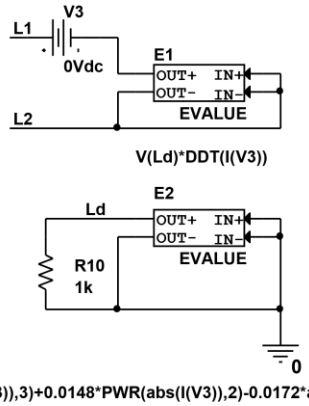

Fig. 6 PSPICE implementation of $L_d(i)$ PSPICE model by applying (14) using the derivative (DDT) operator.

IV. SIMULATION EXAMPLES

Once in the SPICE simulation environment, the models can be used not only to predict the in-circuit physical behavior of a current dependent inductor but also to extract information which is not given in datasheets. For example, the proposed SPICE models can be used to plot the shape of the B-H curve of the cores. This can be done by feeding a time variable signal at the input of the SPICE model and plotting the integral of the input voltage (which is proportional to B) as a function of the current (which is proportional to H). A possible simulation set up for this case is depicted in Fig. 7. It includes the L_d SPICE model, a current ramp generator feeding the model, and a behavioral voltage source that integrates the voltage across the model's input terminals. The resulting 'B-H' curve (Fig. 8) has of course arbitrary units, since the dimension of the core and the number of turns are unknown. If these are available, the actual 'B-H' curve can be reconstructed.

To illustrate the equivalency of the proposed SPICE models, all the models (two L_t and one L_d based) were exposed to same current drive (Fig. 9, lower trace) and the voltages of all the inductor models were recorded (Fig. 9, upper trace). As can be observed, the response of all the models is identical.

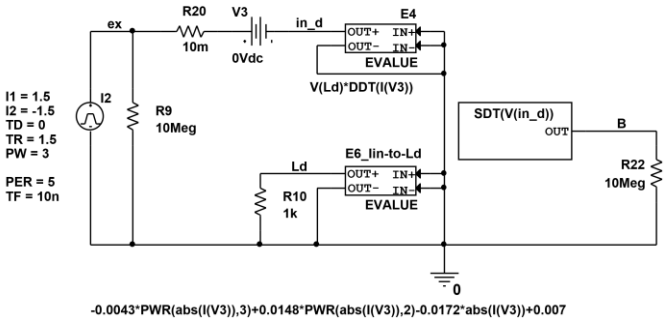

Fig. 7 Simulation set up for B-H extraction.

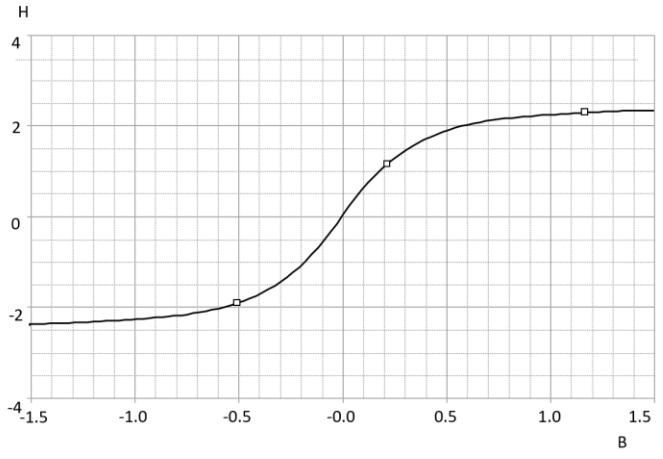

Fig. 8 Results of B-H (arbitrary units) extraction by the SPICE circuit of Fig. 7.

V. EXPERIMENTAL

A ferrite toroid (TX29/19/7.6, Ferroxcube) was used to illustrate the behavior of the proposed inductor models and to validate the SPICE emulation experimentally. The fact that the core has no gap makes it possible to reach the saturation region by a relatively small bias current. To simplify the small signal measurements under bias current, the core was equipped with two windings, 10 turns each. A high impedance current source, built around a MOSFET (IPP045N10N3, Infineon) was used for biasing to avoid the loading of the tested winding by the bias winding. The test circuit for inductance measurements (Fig. 10a) included two voltage power supplies, and an LCR meter. A modified circuit was used for large signal measurements (Fig. 10b). In this case, only one winding was used and a resistor-diode clamping network was added for the discharge duration. The MOSFET was driven by short pulses produced by the pulse generator in the range of several microseconds and the current was measured by a current probe.

Applying LCR meter, the inductance was measured at 10 kHz for a range of bias currents. The results (Fig. 11) were then fitted to an empirical equation displayed in the figure. This equation was used in the proposed L_d SPICE model.

The experimental set up of Fig. 10b was used to expose the inductor to voltage pulses of various length such that the current produced will reach different peak values. The purpose was twofold: to illustrate the large signal behavior of the proposed SPICE models and to verify the concept of energy related inductance (L_e).

Typical reposes of the large signal tests are depicted in Fig. 12. The plots of Fig. 12 clearly show the nonlinear behavior the experimental inductor, caused by the change in the permeability with the bias current.

These measured data can be used to calculate the energy stored in the inductor during charging, and the energy released during discharging. This was done by integrating the product $v * i$ (the inductor current times the inductor voltage), as displayed in Figure 13 for the data of Fig. 12.

Figure 13a depicts the energy stored up to when the peak current is reached, and then released from the inductor passed the peak current. In this case the losses are apparently small and the energy curve returns to zero level. However, in Fig. 13b, the accumulated energy does not return to zero level.

The offset is due to imbalance between stored and released energy, that is, due to losses. Applying trial and error, an equivalent parasitic resistance that will account of the lost energy was found to be 0.5Ω. Using this estimated value, the energy loss was also calculated (Fig. 13b). As seen, the sum of the energy lost plus remaining energy is indeed equal to the energy inputted to the inductor.

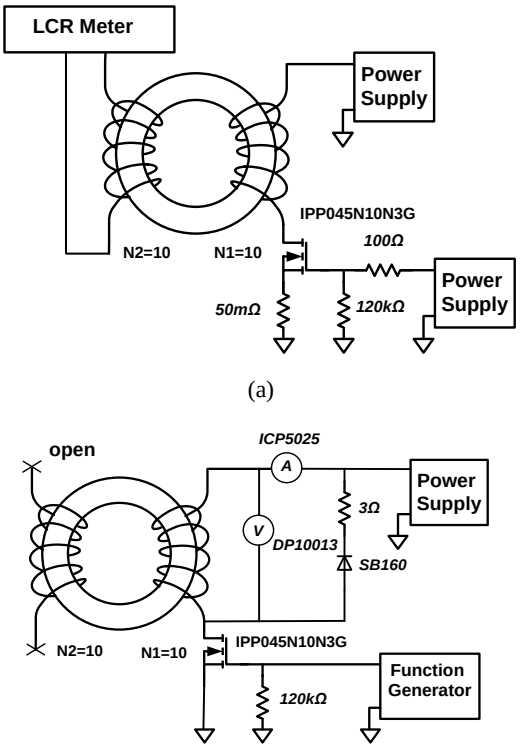

Fig. 10 Experimental set up. (a) For extracting L_d. (b) For large signal tests.

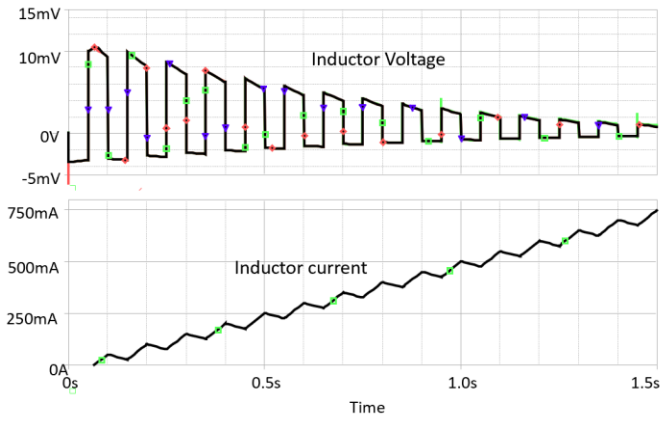

Fig. 9 Terminal voltage of all 3 proposed inductor SPICE models (upper, 3 superimposed traces) to same excitation current (lower trace).

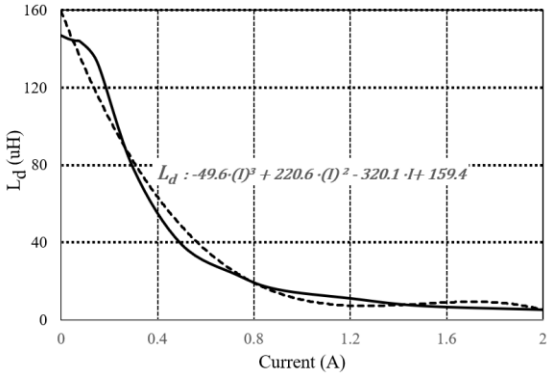

Fig. 11 Measured (solid line) and fitted (dotted line) of L_d as function of bias current. Inductor: TX29/19/7.6 core with 10 turns.

Applying the proposed model of Fig. 6, the experiment of Fig. 12 was simulated by the SPICE circuit depicted in Fig. 14. The circuit includes the basic L_d inductor model plus two behavioral sources that calculate, on the fly, the energy of the inductor plus loss (ET) and the energy lost to the assumed parasitic resistance of 0.5Ω (ER). The first attempt to emulate the experiment by simulation showed a discrepancy between measured and simulated values. It is believed that this disagreement is due to imprecise or unstable values of the inductance, perhaps due to hysteresis. Applying, the current rise slope of Fig. 12a which is within the almost linear section of L_d, a correction factor was calculated and applied to adjust the L_d value. Fig. 15 depicts the simulation results with the corrected L_d.

Furthermore, by applying L_e= 120uH, that was calculated from L_d by (26), we find that the estimated peak stored energy corresponding to Fig. 12b is about 15uJ while the measured (Fig. 13) and simulated one (including about 2uJ losses), per Fig. 15, is about 20uJ. Considering the uncertainty in L_d measurements, this data do confirm the concept of L_e, as well as the ability of the proposed SPICE models to emulate the electrical behavior of the a physical current dependent inductor.

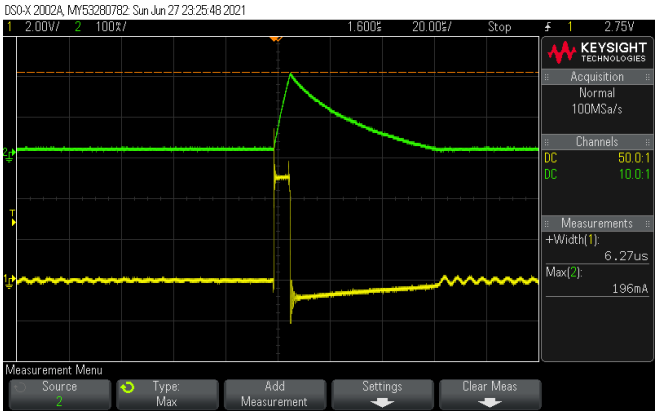

(a)

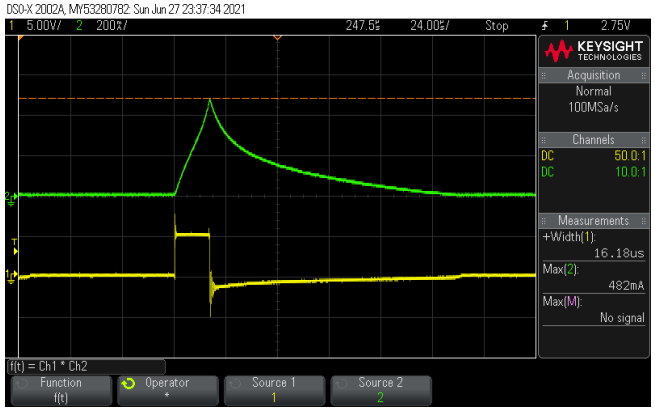

(b)

Fig. 12 Large signal test results for two voltage pulse widths. Lower trace: pulse voltage. Upper trace: inductor current. a: Current, 0.1A/div, voltage 1V/div., horizontal scale 20us/div. b: Current, 0.2A/div, voltage 5V/div., horizontal scale 24us/div.

Considering the uncertainty in the inductance measurements, the simulation results of Fig. 15 seem to verify the correctness of the proposed models of current dependent inductors.

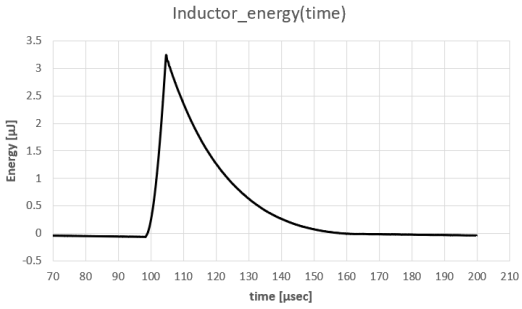

(a)

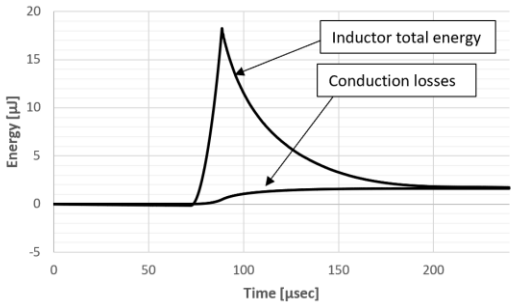

(b)

Fig. 13 Energy charged and discharged during the experiments of Fig. 12.

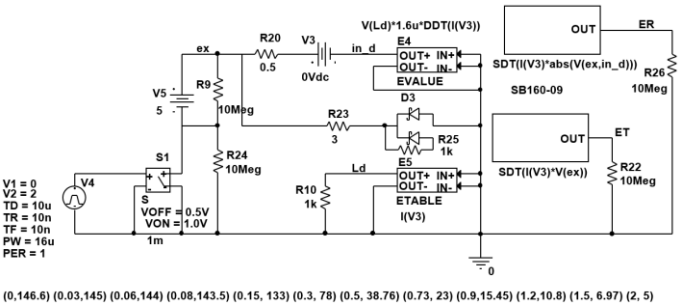

Fig. 14 A SPICE model to emulate the experimental results of Fig. 12.

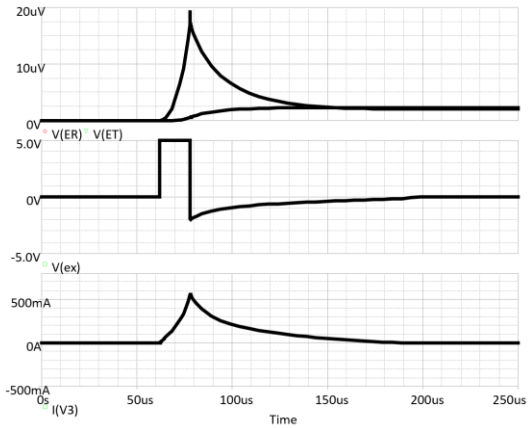

Fig. 15 Simulation results emulating the experiments of Figs. 12b, 13.

VI. Conclusion

The inductance of current dependent inductors can be defined in three ways, as 'total inductance', L_t, 'derivative inductance', L_d and 'energy related inductance' L_e. Of these, the most popular one for which manufacturers normally provide data is L_d. The newly introduced L_e must be used when calculating the energy stored in a nonlinear inductor by the classical equation $E = I^2 \mathrm{L}\,/2$. The study shows that large errors are expected if L_d or L_t are used in the energy calculation.

Starting with the general behavior of the B-H curve of ferromagnetic material, the three inductances where formally defined and their state equations were derived. It is shown that SPICE compatible behavioral models of current dependent inductors can be based on L_t or L_d in a number of variations. Some have a voltage dependent source at the input terminals of the emulated inductor, while other have a current dependent source. It was found, as in [8], that convergence problem during simulation is less likely when the voltage source types are driven by a current source and vice versa.

The equivalency of the various models was demonstrated by examining their responses when they were driven by identical large signals. The validity of the models was verified experimentally by exposing an inductor to a large signal excitation and comparing the resulting response to the one obtained by simulation. The experimental part also tested the applicability of the new L_e concept. Good agreement was found between the analytical expressions, simulations and experimental results. This inductor state space models can be based on (7) or (14) provided that the right 'inductance' is applied.

References

[1] M. Lodi, A. Oliveri and M. Storace, "Behavioral Models for Ferrite-Core Inductors in Switch-Mode DC-DC Power Supplies: A Survey," *2019 IEEE 5th International forum on Research and Technology for Society and Industry (RTSI)*, 2019, pp. 242-247.

[2] L. Mandache, D. Topan, M. Iordache, L. Dumitriu and Ioana Gabriela Sirbu, "On the time-domain analysis of analog circuits containing nonlinear inductors," *2011 20th European Conference on Circuit Theory and Design (ECCTD)*, 2011, pp. 98-101.

[3] B. Evstatiev, D. Kiriakov and D. Trifonov, "Model for Simulation of Nonlinear Inductors in Virtual Environments," *2019 16th Conference on Electrical Machines, Drives and Power Systems (ELMA)*, 2019, pp. 1-4.

[4] Z. Liu, A. Abou-Alfotouh and M. Wilkowski, "Nonlinear inductor modeling for power converter," *2012 Twenty-Seventh Annual IEEE Applied Power Electronics Conference and Exposition (APEC)*, 2012, pp. 1868-1871.

[5] E. Rozanov and S. Ben-Yaakov, "A SPICE behavioral model for current-controlled magnetic inductors," *2004 23rd IEEE Convention of Electrical and Electronics Engineers in Israel*, 2004, pp. 338-341.

[6] W. G. Hurley, W. H. Wölfle, *Transformers and Inductors for Power Electronics: Theory Design and Applications*, John Wiley & Sons, 2013.

[7] L. Zhang, W. G. Hurley and W. H. Wölfle, "A New Approach to Achieve Maximum Power Point Tracking for PV System With a Variable Inductor," in *IEEE Transactions on Power Electronics*, vol. 26, no. 4, pp. 1031-1037, April 2011.

[8] I. Zeltser and S. Ben-Yaakov, "On SPICE Simulation of Voltage-Dependent Capacitors," in *IEEE Transactions on Power Electronics*, vol. 33, no. 5, pp. 3703-3710, May 2018.